PERFORMANCE ANALYSIS OF THE UNCONSTRAINED FXLMS ALGORITHM FOR ACTIVE NOISE CONTROL

Yu Gong

School of Electrical Electronic Engineering
Queen's University of Belfast
Belfast BT9 5AH, UK.

Ying Song and Senjin Liu

Institute for Infocomm Research
21 Heng Mui Keng Terrace
Singapore 119613

ABSTRACT

This paper analyzes the performance of the unconstrained FxLMS algorithm for active noise control (ANC), where we remove the constraints on the controller that it must be causal and has finite impulse response. It is shown in this paper that the unconstrained FxLMS algorithm always converges to, if stable, the true optimum filter even if the estimation of the secondary path is not perfect, and its final Mean Square Error is independent to the secondary path. Moreover we show that the sufficient and necessary stability condition for the feed-forward unconstrained FxLMS is that the maximum phase error of the secondary path estimation must be within 90°, which is only the necessary condition for the feedback unconstrained FxLMS. The significance of the analysis on a practical system is also discussed. Finally we show how the results obtained in this paper can guide us to design a robust feedback ANC headset.

1. INTRODUCTION

The Filter-x LMS (FxLMS) algorithm is usually used in ANC to adapt the coefficients of the controller [1]. The block diagram of the FxLMS algorithm for ANC is shown in Figure 1, where $x(n)$ is the reference input, $d(n)$ is the disturbance signal, $e(n)$ is the residual error, $W(z)$ is the transfer function of the controller, $G(z)$ is the plant transfer function of the secondary path and $\hat{G}(z)$ is the estimate of $G(z)$. In the feed-forward ANC, $x(n)$ is from a separate reference source, while in the feedback ANC, $x(n)$ is synthesized from the feedback of the error signal $e(n)$.

The FxLMS algorithm requires good estimate of $G(Z)$, as otherwise the system may become unstable. Wang and Ren showed in [2] that the sufficient, but not necessary, condition for stability of the feed-forward FxLMS is that the maximum phase difference between $G(z)$ and $\hat{G}(z)$ must not exceed 90°, and Elliott showed

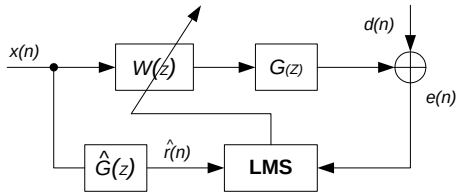

Figure 1: The FxLMS algorithm for ANC

in [1] that this 90° condition is also necessary if the disturbance is pure harmonic. A recent paper [3] tries to show that the 90° condition is not only sufficient but also necessary for the feed-forward FxLMS algorithm. The result is however invalid because that paper implicitly assumed that the disturbance and the reference are totally linear dependent which is not always true in practice. All these analysis, in general, are for feed-forward FxLMS. For the feedback FxLMS, the stability problem becomes complicated and the analysis is normally based on numerical methods such as Nyquist plot [1].

On another front, if we remove the practical constraints on the controller that it must be causal and have finite number of coefficients, both the feed-forward and feedback FxLMS can be analyzed. Elliott analyzed the unconstrained optimum ANC controller but not the FxLMS algorithm. It is shown in this paper that the unconstrained FxLMS tap-weight, if stable, converges to the true optimum tap weight even if the estimate of $G(z)$ is not perfect, and the final Mean Square Error (MSE) is irrelevant to $G(z)$. Moreover we also show that the 90° condition mentioned in the previous paragraph is not only the sufficient but also the necessary condition for the feed-forward unconstrained FxLMS to be stable, and is only the necessary stability condition for the feedback unconstrained FxLMS.

The analysis for the unconstrained FxLMS is very instructive for understanding the algorithm, which oth-

erwise could not be easily obtained. The significance of the analysis for unconstrained FxLMS on practical system is discussed in this paper. In many applications, even the unconstrained optimum controller may approximately be causal and have finite tap length, and the results in this paper are good references in analyzing such systems. An extreme case is when the disturbance is purely harmonic, the unconstrained optimum filter becomes a causal FIR filter, and the analysis in this paper can be directly applied. Finally in this paper, we show how the analysis successfully guide us to construct a robust feedback ANC headset.

2. FEED-FORWARD FXLMS ALGORITHM

The adaptation rule for the FxLMS is known as

$$\mathbf{w}(n+1) = \mathbf{w}(n) - \mu e^*(n)\hat{\mathbf{r}}(n), \tag{1}$$

where μ is the adaptation step-size, $e(n) = d(n) + \mathbf{w}^{\mathrm{H}}(n)\mathbf{r}(n)$, $r(n) = g(n) \otimes x(n)$, $\hat{r}(n) = \hat{g}(n) \otimes x(n)$, $g(n)$ and $\hat{g}(n)$ are the impulse responses of $G(z)$ and $\hat{G}(z)$ respectively.

If the algorithm is stable, (1) converges to (see [1])

$$\mathbf{w}_\infty = -\left(\mathrm{E}[\hat{\mathbf{r}}(n)\mathbf{r}^{\mathrm{H}}(n)]\right)^{-1}\mathrm{E}[\hat{\mathbf{r}}(n)d^*(n)], \tag{2}$$

where $\mathbf{w}_\infty$ is called the *converged solution* which is generally not equal to the optimum solution $\mathbf{w}_{\mathrm{opt}}$ unless $\hat{G}(z) = G(z)$. Subtracting $\mathbf{w}_\infty$ from both side of (1) and taking the expectation, we can obtain the average tap-weight error recursive equation as

$$\mathrm{E}[\mathbf{w}(n+1)-\mathbf{w}_\infty] = [\mathbf{I} - \mu\mathrm{E}[\hat{\mathbf{r}}(n)\mathbf{r}^{\mathrm{H}}(n)]]\cdot\mathrm{E}[\mathbf{w}(n)-\mathbf{w}_\infty]. \tag{3}$$

It is clear from (3) that the average transient behaviour of the FxLMS algorithm is determined by the eigenvalue spread of $\mathrm{E}[\hat{\mathbf{r}}(n)\mathbf{r}^{\mathrm{H}}(n)]$. It is not straightforward, however, to relate the eigenvalues with the plant model error in which we are interested.

In stead of updating the estimated instantaneous gradient term at every sample time as shown in (1), a more accurate estimate is to average over the last N samples and update the tap coefficient in one step. This leads to frequency domain approach of the FxLMS algorithm which is given by [1, Chapter 3]

$$w_i(m+1) = w_i(m) - \mu\mathrm{IFFT}\{E_m^*(k)\hat{R}_m(k)\}_+, \tag{4}$$

where $\{\}_+$ denotes that only the causal part of the IFFT is used, $w_i(m)$ is the ith element of $\mathbf{w}(m)$, $E_m(k)$ and $\hat{R}_m(k)$ are the Fourier Transforms of $e(n)$ and $\hat{r}(n)$ for block m respectively.

It has been shown in [4] that the two strategies of (1) and (4) have similar transient behaviours. Thus we only need to analyze one of them, whichever is easier. In this paper, our analysis is mostly based on the frequency-domain approach.

3. UNCONSTRAINED FXLMS ALGORITHM

In this section, we remove the constraints that the controller must be causal and have finite impulse response, and derive the so-called unconstrained FxLMS algorithm.

By assuming w_i extend from $i = -\infty$ to ∞, $\{\}_+$ can be removed from (4). Taking Fourier Transform on both sides of (4) gives

$$W_{m+1}(k) = W_m(k) - \mu E_m^*(k)\cdot\hat{R}_m(k), \tag{5}$$

where $W_m(k)$ is the Fourier Transform of $w(n)$ for block m,

$$\begin{aligned} E_m(k) &= D_m(k) + W_m(k)R_m(k), \\ R_m(k) &= G_m(k)\cdot X_m(k), \\ \hat{R}_m(k) &= \hat{G}_m(k)\cdot X_m(k), \end{aligned} \tag{6}$$

$G_m(k)$, $\hat{G}_m(k)$, $X_m(k)$ and $D_m(k)$ are the Fourier Transforms of $g(n)$, $\hat{g}(n)$, $x(n)$ and $d(n)$ for block m respectively.

On another front, if $W(z)$ has infinite impulse response, (2) can be expanded as

$$\sum_{l=-\infty}^{\infty} w_\infty(l)\cdot\phi_{\hat{r}r}(i-l) = -\phi_{\hat{r}d}(i), \tag{7}$$

where $\phi_{\hat{r}r}(i-l) = \mathrm{E}[\hat{r}(n-l)r^*(n-i)]$ and $\phi_{\hat{r}d}(i) = \mathrm{E}[\hat{r}(n-i)d^*(n)]$. Taking Fourier Transform on both sides of (7) gives

$$\Phi_{\hat{r}r}(k)\cdot W_\infty(k) = -\Phi_{\hat{r}d}(k), \tag{8}$$

where $\Phi_{\hat{r}r}(k)$ is the cross-power spectrum density between $\hat{r}(n)$ and $r(n)$, and $\Phi_{\hat{r}d}(k)$ is the cross-power spectrum density between $\hat{r}(n)$ and $d(n)$. But $\Phi_{\hat{r}r}(k)$ and $\Phi_{\hat{r}d}(k)$ can also be obtained by

$$\begin{aligned} \Phi_{\hat{r}r}(k) &= \mathrm{E}[\hat{R}(k)R^*(k)] \\ \Phi_{\hat{r}d}(k) &= \mathrm{E}[\hat{R}(k)D^*(k)]. \end{aligned} \tag{9}$$

Substituting (9) into (8) gives

$$\mathrm{E}[\hat{R}(k)R^*(k)]\cdot W_\infty(k) = -\mathrm{E}[\hat{R}(k)D^*(k)]. \tag{10}$$

Further substituting (6) into (10), and assuming that $G(k)$ and $\hat{G}(k)$ are slow varying and irrelevant to $X(k)$, we obtain the *normal equation* of the unconstrained FxLMS filter as

$$\hat{G}(k)G^*(k)\Phi_{xx}(k)W_\infty(k) = -\hat{G}(k)\Phi_{xd}(k), \tag{11}$$

where $\Phi_{xx}(k) = \mathrm{E}[|X(k)|^2]$ is the power spectrum density of $x(n)$, and $\Phi_{xd}(k) = \mathrm{E}[X(k)D^*(k)]$ is the cross power spectrum density between $x(n)$ and $d(n)$.

4. PERFORMANCE ANALYSIS

The converged tap weight and final MSE that the unconstrained FxLMS filter can eventually achieve are derived in this section, followed by the stability analysis for the modelling error of the secondary path. Finally the significance of the analysis on practical systems is discussed.

4.1. Converged Tap Weight And MSE

If $\hat{G}(k) \neq 0$, (11) becomes

$$G^*(k)\Phi_{xx}(k)W_\infty(k) = -\Phi_{xd}(k). \tag{12}$$

Since (12) is independent of $\hat{G}(k)$, the final tap weight to which the unconstrained FxLMX converges must be equal to the true optimum tap weight even if the estimate of the secondary path is not perfect, i.e. $\hat{G}(z) \neq G(z)$.

Moreover the final MSE of the unconstrained FxLMS can achieve is given by, according to Figure 1,

$$\mathrm{E}[|E_\infty(k)|^2] = \Phi_{dd}(k) - |G(k)|^2|W_\infty(k)|^2\Phi_{xx}(k), \tag{13}$$

where $\Phi_{dd}(k) = \mathrm{E}[|D(k)|^2]$ is the power spectrum density of $d(n)$. Again if $\hat{G}(k) \neq 0$, and further assuming that $G(k)$ and $\Phi_{xx}(k)$ are not zeros, from (11) and (13), we have

$$\mathrm{E}[|E_\infty(k)|^2] = \Phi_{dd}(k) - \frac{|\Phi_{xd}(k)|^2}{\Phi_{xx}(k)}. \tag{14}$$

It is interesting from (14) that $\mathrm{E}[|E_\infty(k)|^2]$ does not depend on $G(k)$, implying that even if there exists secondary path $G(Z)$ in the ANC system, it has no effects on the final MSE if the tap-weight is unconstrained.

4.2. Stability Analysis

Noting (10), subtracting $W_\infty(k)$ from both sides of (5) and taking expectation values, and using the independent assumption, we obtain the average weight error behaviour for the unconstrained FxLMS algorithm in frequency domain which is given by

$$\begin{aligned}
&\mathrm{E}[W_{m+1}(k) - W_\infty(k)] \\
&\quad = \left[1 - \mu\mathrm{E}[\hat{R}_m(k)R_m^*(k)]\right] \cdot \mathrm{E}[W_m(k) - W_\infty(k)] \\
&\quad = [1 - \mu\hat{G}(k)G^*(k) \cdot \Phi_{xx}(k)] \cdot \mathrm{E}[W_m(k) - W_\infty(k)].
\end{aligned} \tag{15}$$

It is clear from (15) that, to achieve stability, we must ensure

$$\left|1 - \mu\mathrm{E}[\hat{G}(k)G^*(k)] \cdot \Phi_{xx}(k)\right| < 1. \tag{16}$$

Solving inequality (16) gives

$$0 < \mu < \frac{2 \cdot \mathrm{Re}[\hat{G}(k)G^*(k)]}{|\hat{G}(k)G^*(k)|^2 \cdot \Phi_{xx}(k)}. \tag{17}$$

Therefore from (17), providing that μ is properly set, we obtain the necessary and sufficient conditions for the feed-forward FxLMS to converge which is given by,

$$\mathrm{Re}[\hat{G}(k)G^*(k)] > 0, \tag{18}$$

which is equivalent to $|\theta| < 90°$, where θ the phase difference between $G(k)$ and $\hat{G}(k)$.

4.3. Practical Systems

In practice, the controller of the ANC system is generally a causal FIR filter, and cannot control the whole spectrum of the disturbance as much as the unconstrained controller. Thus generally, the FxLMS in practice has higher final MSE than the unconstrained algorithm. For the practical FxLMS, it is somehow equivalent to have an extra disturbance at the unconstrained FxLMS input to make it have the same performance as the practical FxLMS. By noting this, the stability condition for the practical FxLMS algorithm becomes

$$\mathrm{Re}[\hat{G}(k)G^*(k)] + \Delta(k) > 0, \tag{19}$$

where $\Delta(k) \geq 0$. Therefore at the frequencies where $\Delta(k) > 0$, even if the phase error exceeds 90°, the system can still be stable. This observation was also implied in [2] which showed that $\mathrm{Re}[\hat{G}(k)G^*(k)] > 0$ is the sufficient but not necessary condition for the stability of the feed-forward FxLMS algorithm, which indirectly ensures the reliability of (19).

Eqn. (19) can also be used as a criterion for comparing different robust FxLMS algorithms, since all robust FxLMS eventually have stable conditions in form of (19). The larger the $\Delta(k)$ is, the bigger the *stability margin* the algorithm has, but the poorer the disturbance reduction performance it achieves. For example, the leaky FxLMS algorithm [1] introduces a leaky factor in the adaptation rule, and the weight-constrained FxLMS algorithm [5] constrains the norm of the tap-weight. Both approaches achieve robustness by introducing an equivalent $\Delta(k)$ in the stable condition similar to (19), where the one that has larger $\Delta(k)$ for the same final MSE is better than the other in the sense of robustness. The analytical derivation of $\Delta(k)$, however, can not always be obtained, and numerical methods have to be used.

5. A ROBUST FEEDBACK ANC HEADSET

In this section we show how the analysis obtained above are useful to design a real-time robust feedback ANC headset. The stability analysis of the feedback FxLMS algorithm is difficult to obtain as mentioned in [1]. Following the same procedure as in section 4.2, however, at least we can show that the necessary, but not the sufficient, stability condition for the unconstrained feedback FxLMS algorithm is the same as that for its feed-forward counterpart, which is (18). For practical feedback FxLMS, though (18) may not be a necessary condition, violating (18) leads to small *stability margin* which again forces the algorithm to converge slowly. Consequently we should ensure the phase error to be within 90° for the feedback FxLMS algorithm.

Feedback FxLMS algorithm can be used in the ANC headset to generate a quiet zone around the human ear. When the headset's position is fixed, the transfer function $G(z)$ varies little and can be well estimated. Usually $G(z)$ is measured when the headset is put on the ear, and at this time we can assume $G(z) \approx \hat{G}(z)$. When the headset is pulled away from the ear, however, $G(z)$ changes dynamically. The phase change of the transfer function due to the headset position variation is measured as shown in Figure 2. This measured phase difference is approximately equal to the phase error of $G(z)$ and $\hat{G}(z)$ for the case when the headset is away from the ear, and thus influences the stability of the headset when it is at this position.

In our experiments, at first an ANC headset was set up using only digital feedback loop. However the system always became unstable when the headset was pulled away from the ear. Plotting the phase change of the transfer function as shown in Figure 2(a), it was found that, based on the analysis in this paper, the instability was due to that the phase errors at some frequencies exceed 90°. To overcome this problem, an analog feedback loop, in parallel to the digital one, is added to the system. This arrangement effectively reduced the phase fluctuation of the transfer functions as shown in Figure 2(b), where phase variations were limited to be within 90°. Together with other appropriate system design, a robust feedback ANC headset was then designed, though at some frequencies the phase errors approach very closely to 90°.

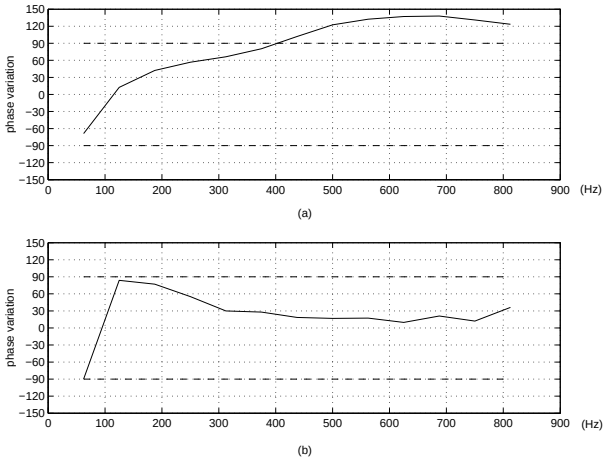

Figure 2: Secondary path phase change due to the headset position variation. (a) Phase change when there is only digital feedback loop in the ANC; (b) Phase change when an analog feedback loop is added to the ANC headset.

6. CONCLUSION

This paper analyzes the performance of the unconstrained FxLMS algorithm for ANC, where both feedforward and feedback ANC are considered. We show that the unconstrained FxLMS filter converges, if stable, to the true optimum filter even if the estimate of $G(z)$ is not perfect, and its final MSE is irrelevant to $G(z)$. More importantly, we show that for feed-forward unconstrained FxLMS, the sufficient and necessary stability condition is that the maximum phase error of the secondary path estimation must be within 90°, which is however only the necessary condition for the feedback unconstrained FxLMS. Finally we illustrate how the analysis in this paper successfully guides us to set up a robust feedback ANC headset.

REFERENCES

[1] S. J. Elliott, *Signal Processing for Active Noise Control*, Academic Press, London, 2001.

[2] A. K. Wang and W. Ren, "Convergence analysis of the multi-variable filtered-s LMS algorithm with application to active noise control," *IEEE Transactions on Signal Processing*, vol. 47, pp. 1166–1169, 1999.

[3] Y. Kajikawa, J. Yabuki, and Y. Nomura, "Stable condition considering modelling error in the fitlered-X LMS algorithm," in *IEEE International Symposium on Circuit and Systems*, Geneva, Switzerland, May 2000.

[4] S. J. Elliott and P. A. Nelson, "Algorithms for the active control of periodic sound and vibration," in *ISVR Technical Memorandum, No. 679*, University of Southampton, UK, 1986.

[5] H. Lan, M. Zhang, and W. Ser, "A weight-constrained FxLMS algorithm for feedforward active noise control systems," *IEEE Signal Processing letters*, vol. 9, no. 1, 1999.